



# Kinetic modelling and mechanism elucidation of catalyst-free dimethyl terephthalate hydrolysis process intensification by reactive distillation

Žan Lavrič<sup>a,b</sup>, Aleksa Kojčinović<sup>a,b</sup>, Irina Yarulina<sup>c</sup>, Manfred Stepanski<sup>c</sup>, Blaž Likozar<sup>a</sup>, Miha Grilc<sup>a,b,\*</sup>

<sup>a</sup> Department of Catalysis and Chemical Reaction Engineering, National Institute of Chemistry, Hajdrihova 19, SI-1000, Ljubljana, Slovenia

<sup>b</sup> University of Nova Gorica, Vipavska 13, SI-5000, Nova Gorica, Slovenia

<sup>c</sup> Sulzer Chemtech Ltd., Neuwiesenstrasse 15, 8401, Winterthur, Switzerland

## ARTICLE INFO

Handling Editor: Jian Zuo

### Keywords:

PET recycling  
Hydrolysis  
Kinetic modelling  
Reactive distillation  
Process optimization

## ABSTRACT

Polyethylene terephthalate (PET) is a widely used thermoplastic polymer in the packaging and materials industries, and is predicted to have continuous market growth in the future. Methods such as glycolysis and methanolysis of PET have been identified as promising approaches in sustainable chemical recycling of PET. The latter produces dimethyl terephthalate (DMT), which can be easily hydrolyzed to terephthalic acid (TPA) at elevated temperatures and pressures, and further reused for PET production. The aim of this study was to develop a kinetic model for the hydrolysis of dimethyl terephthalate, using the experimental data. Various reaction conditions (temperature, pressure, time) have been investigated and used to calculate the activation energies and reaction rate constants, while the variation in reactor setup with methanol (MeOH) removal was conducted to show its detrimental effect on the efficiency of the reaction and selectivity towards terephthalic acid. The first reaction step of DMT to monomethyl terephthalate (MMT) is relatively irreversible, while the second reaction step of MMT to TPA ceases, as soon as the equilibrium is reached. Highest yields of TPA (76.7 %) were obtained after 40 min at 265 °C, with MeOH removal, and the activation energy was calculated to be 95 and 64 kJ mol<sup>-1</sup> for the first and second hydrolysis reaction step, respectively.

## 1. Introduction

Polyethylene terephthalate (PET) is a widely used thermoplastic polymer known for its transparency and semi-crystalline nature, and has extensive applications in the packaging industry, stretch blown moulding bottle manufacturing, and textile fibres (Pudack et al., 2020). The global market for recycled PET technologies is expected to grow from 11.0 billion USD in 2023 to 15.0 billion USD by 2028, propelled by compound annual growth rate of 6.5 %. Market growth is mainly driven by government regulations and new legislation, primarily promoting circular economy practices and the use of recycled materials, as a consequence of increasing global demand for sustainable and environmentally friendly packaging (Aashish Mehra, 2023; "Global Recycled PET Market - 2024–2031," 2024).

Recycling of PET can be classified into four different categories, such as primary, secondary, tertiary and quaternary, which is well described elsewhere (López-Fonseca et al., 2010; Neale et al., 1983; Sinha et al., 2010). Mechanical (secondary) recycling processes requires thorough

pre-sorting and separation of the wastes, size reduction, melt filtration and reforming of the material (Benyathiar et al., 2022). However, the polymer material properties deteriorate with each cycle. On the other hand, chemical recycling includes depolymerization of PET material back to monomers, which can be purified by distillation and drying, and reused again for further polymers manufacturing (Pudack et al., 2020).

Chemical recycling of PET involves various methods, such as hydrolysis (Čolnik et al., 2021; Liu et al., 2012), glycolysis (Zhu et al., 2012a, 2012b) and methanolysis (Genta et al., 2005; Kurokawa et al., 2003); the appeal of these methods lies in their potential for large-scale implementation, which represents a significant step toward addressing the challenges of plastic waste management. From industrial point of view, glycolysis is the most cost-effective process for PET recycling (Baliga and Wong, 1989; Chen et al., 1991). The main advantage of glycolysis is a rather simple integration into a conventional PET production plant, where the recovered bis(2-hydroxyethyl) terephthalate (BHET) can be blended with fresh BHET. The reaction is usually performed under ambient pressures and temperatures in the range of

\* Corresponding author. Department of Catalysis and Chemical Reaction Engineering, National Institute of Chemistry, Hajdrihova 19, SI-1000, Ljubljana, Slovenia.  
E-mail address: [miha.grilc@ki.si](mailto:miha.grilc@ki.si) (M. Grilc).

180–240 °C.

Contrary to glycolysis and BHET formation, methanolysis is the process, where either BHET or PET is mixed with methanol at temperatures of 190–280 °C and pressures of 20–40 bar<sub>g</sub> (Gauge pressure) (Kim et al., 2001; Pudack et al., 2020). During the reaction, dimethyl terephthalate (DMT) and ethylene glycol (EG) are produced. Early PET polymerization process, dating back in 1941, actually utilizes DMT as starting material, since its purity is of high importance and its purification by distillation is rather easy. During 1960s, the purification of terephthalic acid (TPA) was made possible through re-crystallization, and ever since, more than 70 % of global PET production is based on TPA. The main advantage of the TPA route is its well-established industrial processes and supply chains. Currently, PET production primarily uses TPA, causing a decline in DMT production and the shutdown of DMT-to-PET facilities. With the development of PET methanolysis routes, the market may become saturated with DMT, which has limited demand. (“Dimethyl Terephthalate (DMT) & Polyethylene Terephthalate (PET): Navigating Market Changes & Innovations,” 2024)

Another way to produce TPA is through hydrolysis of DMT. The latter, performed either in batches or continuously, results in a final reaction mixture consisting of TPA, methanol (MeOH), monomethyl terephthalate (MMT) and by-products from crude DMT (Pudack et al., 2020). During the hydrolysis process, methyl esters are hydrolyzed, resulting in the formation of a methanol - water mixture. This mixture is further processed for MeOH recovery, where the recovered MeOH is fed to methanolysis, while water is recycled back to the hydrolysis process. The conversion of DMT involves two reactions: the rapid and irreversible conversion of DMT to MMT and the subsequent reversible conversion of MMT to TPA, which has been kinetically described by Sim and coworkers (Sim and Han, 2006). Their study showed the irreversible nature of the first reaction and an established equilibrium between MMT and TPA, in the temperature range of 200–230 °C. The addition of zinc acetate as catalyst improved the final yield of TPA by 20 %. In addition, the reaction was autocatalyzed by TPA, since its proton also acts as an acid catalyst. However, one of the drawbacks of homogeneous catalysis is the separation of the catalyst from the final mixture. Guo et al. (2022) hydrolyzed DMT with Nb-HZSM-5 zeolite, achieving 94 % yield of TPA at 200 °C. Their catalyst showed good stability and was successfully re-used for many cycles with a minor loss of activity. While catalysts enhance TPA's yield, they do not affect the thermodynamics. Following Le Chatelier's principle, the second reaction could be shifted towards TPA and MeOH, if one or both are removed from the reaction mixture, during the reaction.

In this study, the primary objective was to investigate the reaction kinetics of DMT hydrolysis without the addition of any catalyst, based on the experimental data. Our main objective was to investigate the effects of the presence of MeOH in the reaction mixture on the extent of TPA formation. This comparative analysis should reveal the crucial differences and shed light on the underlying mechanisms. Significantly, this study represents the first attempt to determine the kinetics of this high-temperature PET recycling process in catalyst free conditions, providing valuable insight into its fundamental aspects.

## 2. Materials and methods

Materials and equipment used are described in this section, as well as methodology for kinetic modeling. Development of HPLC analysis technique, reactor system design and experimental procedure, TPA degradation tests and NMR measurements of the final solution are presented in the supplementary material.

### 2.1. Materials

Dimethyl terephthalate was purchased from Sigma Aldrich, MMT was purchased from TCI, TPA was purchased from Sigma Aldrich. Methanol was purchased from Merck. All reaction experiments were

performed with deionized water H<sub>2</sub>O (dH<sub>2</sub>O) (18.2 MΩ). Dimethyl sulfoxide (DMSO) was purchased from Honeywell, dimethyl formamide (DMF) was purchased from Supelco, acetonitrile was purchased from VWR Chemicals, formic acid was purchased from Sigma Aldrich. Teflon gaskets, used to seal the reactor, were purchased from Dastafion.

### 2.2. Equipment

Experiments were performed in a high-pressure autoclave system with six parallel reactors (Amar Equipment Pvt. Ltd., Mumbai, India). Each batch system consists of a 250 mL vessel (inner diameter 67 mm and height 80 mm), with a magnetically driven Rushton turbine impeller (diameter 30 mm, 14 mm above the autoclave bottom). The autoclave system is equipped with a separate internal and external cooling system, which ensures adequate temperature control inside each autoclave and for the external parts (sampling lines, head of the impeller). Each autoclave can be operated under independent operating conditions (composition of the reaction mixture, reaction temperature, time and pressure), each in a batch mode. The gas outlet of the reactor was connected to a reflux condenser with independent thermostat (Julabo F25). The reflux condenser was connected to a solid particle trap, to prevent clogging of the gas lines at the outlet of the system. The system is shown in supplementary information in Figure SX (scheme and actual system, respectively). Development of analysis techniques, DMT hydrolysis experiments and TPA degradation and CO<sub>2</sub> analysis of gaseous phase are described in detail in supplementary part of this paper.

### 2.3. Kinetic modelling

In order to develop a kinetic model, both reactions presented in Fig. 1 were included and concentrations of all three, the reactant, the intermediate and the product were considered. Based on low solubility of DMT, MMT and TPA and 25 °C, paper by Takebayashi and coworkers (Takebayashi et al., 2012) clearly shows that at 265 °C the TPA's mass fraction is 0.17. However, in our experiments, the mass fraction of TPA in the solution is 0.12 at 265 °C, which would suggest that the TPA is completely dissolved. Unfortunately, there is no other study of solubility of DMT or MMT at 265 °C in pure water. Although solubilities of DMT and MMT are lower than of TPA at 265 °C, the kinetic model was simplified to account for all compounds being soluble in the whole temperature range. Furthermore, Zhang (Zhang et al., 2013) showed, that water-MeOH mixture improves DMT, MMT and TPA solubility, meaning that while hydrolysis is progressing, the remaining methanol in the liquid phase improves dissolution of DMT, MMT and TPA. In addition,  $P_{xy}$  diagrams for vapour-liquid equilibrium (VLE) were calculated in Aspen Plus for the binary mixture of MeOH and water at all temperatures relevant in this study (235, 250 and 265 °C). The recorded pressures during the reaction were  $34 \pm 1$  bar<sub>a</sub> at 235 °C,  $45 \pm 1$  bar<sub>a</sub> at 250 °C and  $55 \pm 1$  bar<sub>a</sub> at 265 °C. Fig. S3 shows the VLE diagrams derived from Aspen Plus, marked with red lines representing the experimentally measured pressure at each temperature. The data show that the content of the reactor is in a two-phase regime, while the hydrolysis reactions predominantly take place in the liquid phase of the reactor. This was also assumed in the kinetic model.

The purpose of this model is to describe the equilibrium reactions that occur in the liquid phase of the reactor. The concentration of each compound was calculated by solving a set of ordinary differential equations (ODE) based on the reactions shown in Fig. 1.

The temperature data were automatically recorded during the entire length of the experiment and used to calculate the reaction rate constants and the corresponding activation energies at each time step during the simulation. The effect of temperature on the reaction rate constant was calculated using the Arrhenius law, as shown in Eq. (1),

$$k_i(T_{(t)}) = k_i(T_{ref}) \cdot \exp\left(\frac{Ea_i}{R} \cdot \left(\frac{1}{T_{ref}} - \frac{1}{T_{(t)}}\right)\right) \quad (1)$$

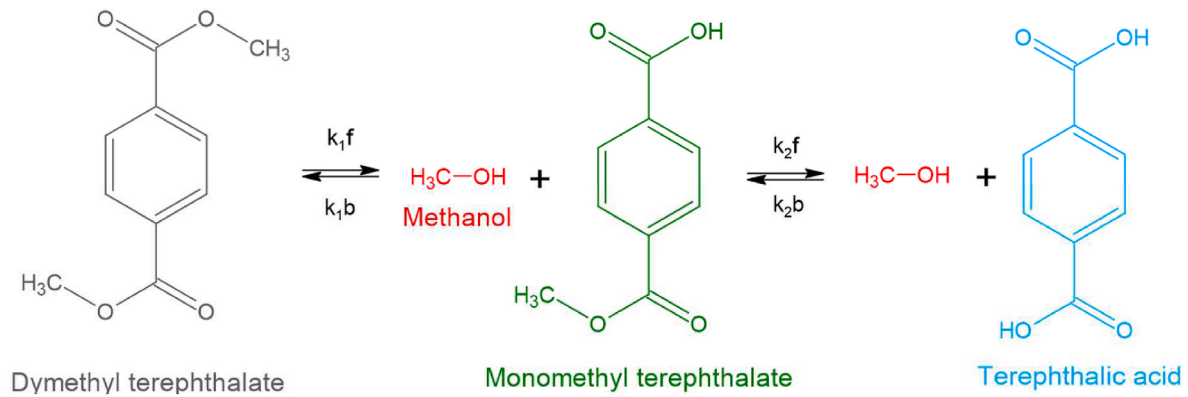


Fig. 1. DMT and MMT hydrolysis reactions.

where  $k_i$  stands for the reaction rate constant of a reaction  $i$  at given time and temperature and  $E_{a_i}$  for the corresponding activation energy.  $T_{ref}$  is a reference temperature of 538 K at which the reaction rate constants are reported (in Table 2),  $R$  is the gas constant ( $8.314 \text{ J mol}^{-1} \text{ K}^{-1}$ ),  $T_{(t)}$  is the recorded temperature at the time of sampling ( $t$ ), while  $C_x$  in below equations (Eqs. (2)–(7)) is the concentration of compound  $x$  (DMT, MMT, TPA, or MeOH) obtained at time  $T_{(t)}$ .

The mass balance equations for DMT, MMT, TPA, and MeOH are presented below. Since water is the solvent and is present in excess, its concentration is omitted from the equation for the hydrolysis reaction rate:

$$\frac{dC_{DMT}}{dt} = -k_1^f \cdot C_{DMT} + k_1^b \cdot C_{MMT} \cdot C_{MeOH} \quad (2)$$

$$\frac{dC_{MMT}}{dt} = k_1^f \cdot C_{DMT} - k_1^b \cdot C_{MMT} \cdot C_{MeOH} - k_2^f \cdot C_{MMT} + k_2^b \cdot C_{TPA} \cdot C_{MeOH} \quad (3)$$

$$\frac{dC_{TPA}}{dt} = +k_2^f \cdot C_{MMT} - k_2^b \cdot C_{TPA} \cdot C_{MeOH} \quad (4)$$

Mass balance for MeOH in the simulation, where MeOH was not removed during the reaction is presented in Eq. (5):

$$\frac{dC_{MeOH}}{dt} = k_1^f C_{DMT} + k_2^f C_{MMT} - k_1^b \cdot C_{MMT} \cdot C_{MeOH} - k_2^b \cdot C_{TPA} \cdot C_{MeOH} \quad (5)$$

The mass balance of MeOH for the experiments where MeOH was removed has an additional term where MeOH is removed from the reaction mixture. This allows its concentration curve to follow the experimentally determined concentration with analysis GC-MS:

$$\frac{dC_{MeOH}}{dt} = k_1^f C_{DMT} + k_2^f C_{MMT} - k_1^b \cdot C_{MMT} \cdot C_{MeOH} - k_2^b \cdot C_{TPA} \cdot C_{MeOH} - r_{MeOH \text{ flush}} \quad (6)$$

The last term in Eq. (6) represents a cumulative contribution of MeOH removal from the liquid phase of the reactor. The rate of MeOH removal from the gas phase is described with Eq. (7a), where  $\dot{V}$  represents the volumetric flow rate,  $V$  is the volume of gas phase and  $C_{MeOH}^{Gas}$  the concentration of MeOH in gas phase.

$$r_{MeOH \text{ flush}} = \frac{\dot{V}}{V} \cdot C_{MeOH}^{Gas} \quad (7a)$$

Similarly, Eq. (7b) represents MeOH mass transfer rate from liquid to gas phase.  $k_{GL}$  represents the mass transfer coefficient,  $a$  is ratio between GL surface area and liquid phase volume,  $He$  is Henry's constant,  $C_{MeOH-liquid}$  is concentration of MeOH in the liquid phase.

$$r_{MeOH L} = k_{GL} \cdot a \cdot (He \cdot C_{MeOH-liquid} - C_{MeOH}^{Gas}) \quad (7b)$$

Since this term is used only when MeOH is removed,  $C_{MeOH}^{Gas}$  is always

lower than the concentration in the liquid phase, imposing the flux of MeOH from liquid to gas to reactor outlet. However, due to the difficult reaction conditions under which the reaction is carried out, it was impossible to determine the exact surface to volume ratio ( $a$ ) or the exact flow rate of  $N_2$  in the system. Hence,  $r_{MeOH \text{ flush}}$  was simplified and used as Eq. (7c) in our model.

$$r_{MeOH \text{ flush}} = k_{flush} \cdot C_{MeOH-liquid} \quad (7c)$$

As can be seen from Eq. (7d),  $k_{flush}$  is proportional to the mass transfer rate ( $k_L$ ) of MeOH at the gas-liquid interface and to Henry's law of MeOH removal from the gas phase of the reactor.

$$k_{flush} \propto k_L \cdot a \cdot He \cdot \frac{\dot{V}}{V} \quad (7d)$$

Matlab R2021b software was used to numerically solve the formulated system. The concentration profiles were solved as a function of time using the ODE23tb solver, an implicit Runge-Kutta formula with trapezoidal rule step as the first stage and a second-order backward differentiation formula as the second stage. The initial concentrations of all compounds were set to zero, except for DMT, which was the starting compound of the reaction mixture.

### 3. Results

DMT hydrolysis has been devised into two subsections. Firstly, representative experiments are shown in subsection 3.1, with corresponding conversions and yields at various experimental conditions. The latter is followed by the kinetic evaluation of the experiments in subsection 3.2, where experimental data were used to extract the relevant kinetic parameters.

#### 3.1. DMT hydrolysis

The hydrolysis of DMT to TPA consists of two successive reactions, where the first reaction can be classified as highly irreversible and the second one as reversible. It can be seen from Fig. 1 that one molecule of MeOH is formed in each reaction step, which affects the reaction rate in the reversible direction. With this in mind, the objective was to perform experiments with and without MeOH removal to determine their effect on the extent of hydrolysis and the final yield of TPA. Table 1 shows the experiments performed during the DMT hydrolysis research.

Experiments 3, 4, and 5 were heated only to the target temperatures of 235 °C, 250 °C, and 265 °C, respectively. Experiments 6–11 were performed as a continuation of experiments 3, 4, and 5 once the target temperature was reached. No MeOH removal was initiated at this time. Experiments 12–16 were conducted at 265 °C, and MeOH removal was performed by introducing  $N_2$  into the gas phase of the reactor and simultaneously removing MeOH from the gas phase. That is, when the target temperature was reached (~30 min), the valves at the inlet of the

**Table 1**  
Overview of the experimental runs.

	Exp No.	$m_{DMT}$ [g]	$V_{H_2O}$ [L]	$T_{target}$ [°C]	$p_{init. N_2}$ [bar <sub>g</sub> ]	$T_{reflux}$ [°C]	$T_{cond.}$ [°C]	$t_{heating}$ [min]	$t_{reaction}$ [min]	$N$ [min <sup>-1</sup> ]
Heating to 265 °C	3	10.0	0.06	235	10	90	2	23	0	600
	4	10.0	0.06	250	10	90	2	26	0	600
	5	10.0	0.06	265	10	90	2	30	0	600
No MeOH removal	6	10.0	0.06	235	10	90	2	19	15	600
	7	10.0	0.06	235	10	90	2	19	30	600
	8	10.0	0.06	250	10	90	2	27	15	600
	9	10.0	0.06	250	10	90	2	27	30	600
	10	10.0	0.06	265	10	90	2	31	15	600
	11	10.0	0.06	265	10	90	2	31	30	600
MeOH removal	12	10.0	0.06	265	10	90	2	30	5	600
	13	10.0	0.06	265	10	90	2	31	10	600
	14	10.0	0.06	265	10	90	2	30	20	600
	15	10.0	0.06	265	10	90	2	30	30	600
	16	10.0	0.06	265	10	90	2	30	40	600

**Table 2**  
Kinetic parameters and their 95% confidence intervals determined by regression analysis.

Kinetic parameters						
$k_{1f}$ (min <sup>-1</sup> )	$k_{1b}$ (min <sup>-1</sup> )	$k_{2f}$ (min <sup>-1</sup> )	$k_{2b}$ (min <sup>-1</sup> )	$Ea_{1f}$ (kJ mol <sup>-1</sup> )	$Ea_{2f}$ (kJ mol <sup>-1</sup> )	$k_{flush}$ (min <sup>-1</sup> )
$0.228 \pm 0.017$	$<10^{-7}$	$0.151 \pm 009$	$(1.0 \pm 0.1) \bullet 10^{-3}$	$95 \pm 3$	$64 \pm 3$	$0.10 \pm 0.01$

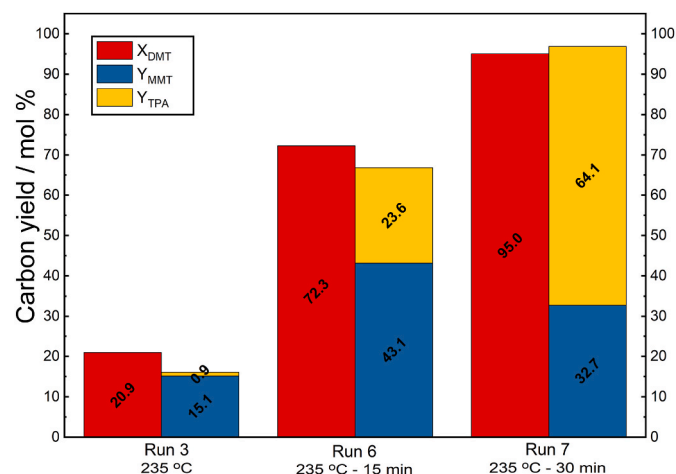
gas phase were opened and the needle valve at the outlet was adjusted to ensure the blow-out of the system and the removal of MeOH.

In Fig. 2, conversion of DMT and yield of MMT and TPA is presented for experiments carried out at the temperature of 235 °C.

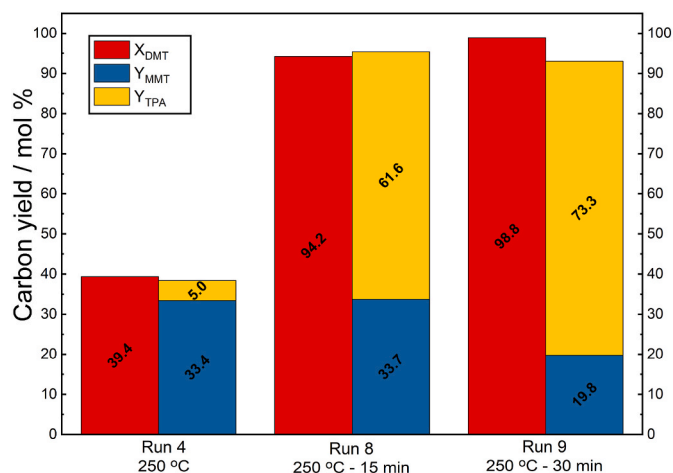
Fig. 2 shows that at a temperature of 235 °C, the conversion of DMT to MMT begins slowly. If the reaction is kept at 235 °C for 15 and 30 min, 72.3 and 95.0% of DMT is converted, respectively. With longer reaction time, the TPA yield increases to 64.1 % and the MMT yield remains at 32.7 %, indicating that either the reaction time needs to be prolonged or the temperature needs to be increased to increase the conversion and yield.

Fig. 3 shows the DMT conversion and MMT and TPA yields obtained from reactions carried out at a temperature of 250 °C. After 15 min of reaction at 250 °C, 94.2% of DMT has been converted.

Since heating the reaction mixture from 235 to 250 °C requires additional time, a comparison between run 7 and run 8 would be relevant because of the similar reaction time. It can be seen that a higher



**Fig. 2.** Conversion of DMT and yields of MMT and TPA for experimental runs at 235 °C.



**Fig. 3.** Conversion of DMT and yields of MMT and TPA for experimental runs at 250 °C.

conversion is achieved at a higher temperature and the TPA yield is also higher (10 %).

To ensure a three-point calibration to determine the activation energies of the reactions, another series of experiments was performed at 265 °C. Fig. 4 shows obtained conversions and yields for these experiments.

At the highest temperature tested and the longest reaction time (run

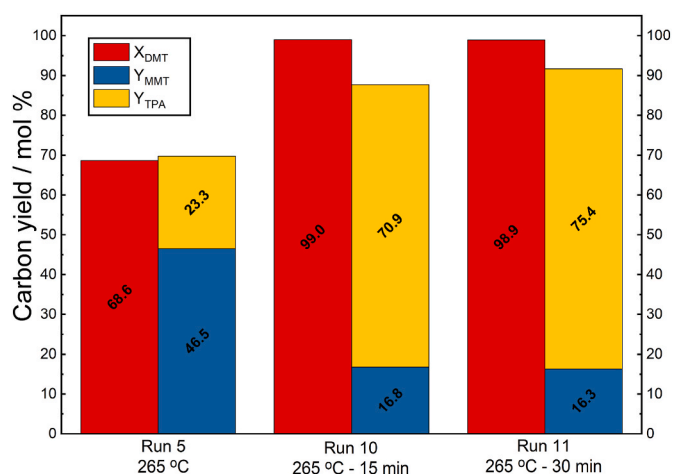


**Fig. 4.** Conversion of DMT and yields of MMT and TPA for experimental runs at 265 °C.

11), 99 % DMT is converted and the highest yield of TPA (75.4 %) is obtained among the experiments where MeOH was not removed from the reaction mixture. Therefore, the experiments with MeOH removal were carried out at a reaction temperature of 265 °C.

To test the effect of MeOH on the equilibrium of the second reaction, 5 additional time points were performed at 265 °C, with continuous removal of the gas phase from the reactor. Fig. 5 shows the conversion and yield for the latter.

The final yield of TPA after 40 min of reaction at 265 °C is similar to run 11, but the yield of MMT decreased significantly. Thus, the removal of MeOH from the reaction mixture forces the equilibrium reaction towards TPA, but also TPA is removed from the system.

### 3.2. Kinetics of DMT hydrolyzation

Kinetic evaluation of DMT hydrolysis was performed using Matlab R2021b, with the experimental data used as a regression anchor for mathematical prediction of the concentration profile of each compound in the liquid reaction mixture.

As mentioned in Section 2.4, a different mass balance equation was used for the experiment, where MeOH removal was performed, by purging the gas phase of the reactor with N<sub>2</sub>. Fig. 6 shows the results of the kinetic regression evaluation.

The concentration profiles show that the reaction is initiated as soon as the temperature is above 200 °C. At 235 °C, both the first and second reactions proceed relatively slow. When the temperature is increased to 250 °C, both reaction rates increase, and at 265 °C the second reaction reaches equilibrium. Table 2 shows the kinetic parameters obtained by regression analysis.

The reaction rate constants for the first and second forward reactions are 0.22 and 0.15 min<sup>-1</sup>, respectively, indicating that the first reaction is faster than the second. Comparing the activation energies, the  $E_a$  of the first reaction is  $95 \pm 3$  kJ mol<sup>-1</sup>, which is higher than that of the second reaction ( $64 \pm 3$  kJ mol<sup>-1</sup>). The contribution of temperature on reverse reactions were considered negligible. With this in mind, and considering the concentration vs. time profile for the reaction with the intermediate MMT, it could be concluded that the first reaction, from DMT to MMT, requires a higher temperature but is relatively fast and non-reversible, while the reaction from MMT to TPA is initiated at lower temperatures but the reversibility is more significant.

After reactions were carried out without MeOH removal, the yield of TPA was highest at a temperature of 265 °C, but it is clear from the concentration profile that the concentration of MMT and TPA is practically the same at 47 and 60 min of reaction time. The results show that when MeOH was removed during the reaction, almost all of the DMT

was converted to TPA. The rate of MeOH removal ( $k_{\text{flush}}$ ) was determined to be 0.1 min<sup>-1</sup>.

The differences between the two experimental set-ups are even more evident from Fig. 7, which shows predicted concentration profiles of compounds of interest, under various reaction conditions. Reaction rate constants and their corresponding activation energies were used to predict MMT, TPA and MeOH concentrations profiles.

The results presented in Fig. 7 clearly show the difference between the various experimental set-ups and the crucial influence of MeOH removal. If MeOH is not removed from the liquid phase, the equilibrium is reached. Extrapolating the reaction temperature and time beyond the experimental framework shows that the yield of MMT decreases from 15.2 % to 8.9 % when the temperature is increased from 265 °C to 290 °C. On the other hand, if MeOH is removed from the reaction, the yield of MMT at the end of the reaction at 265 or 290 °C is practically zero. In addition, the predicted yield at 230 °C, when MeOH is removed from the liquid phase, is actually lower (6.7 %) after 100 min of reaction time than at 290 °C without MeOH removal.

It is important to emphasize here that the concentration points were normalized for the kinetic evaluation. In reality, as it can also be seen in Fig. 6, the TPA yield is lower than expected, but the exact cause of the lower yield has not yet been determined and will be discussed below.

## 4. Discussion

As shown in the present study, the hydrolysis of DMT to TPA depends mainly on one parameter: the extent of removal of MeOH from the reaction mixture during the reaction. The results show that the final yield of TPA is higher when MeOH is removed during the reaction. However, there are still additional aspects that need to be considered in future research.

The bar chart in Fig. 5 shows a discrepancy where the sum of MMT and TPA yields is lower than the expected 99 % DMT conversion. Although the exact cause of this discrepancy is unknown, we suspect several possible scenarios. One possibility is that the carbon balance (CB) is 80–90 % because DMT, MMT, and TPA precipitate as the reactor cools to 50 °C. This results in the loss of each compound during sample preparation.

The CB loss can also be attributed to the sublimation of TPA during the reaction at 265 °C. Kimyonok et al. (Elmas Kimyonok and Ulutürk, 2016) demonstrated that the sublimation of TPA starts to become significant at temperatures above 270 °C. It is important to consider the difficult conditions that prevailed during the experiment. First, the heating jacket temperature is increased to 450 °C and maintained above 400 °C even after the target temperature of 265 °C is reached in the reactor. Due to these harsh conditions, it is possible that TPA sublimates at the same time when MeOH is removed from the reactor. To exclude TPA decompositions, we performed experiments with TPA as reactant at 265 °C, operating in batch configuration, without purging of the reactor's headspace with N<sub>2</sub> (experiment, where MeOH was removed). The results are shown in Fig. 8.

After the  $\mu$ GC analysis of the gas phase sample obtained after the reaction under 265 °C with TPA as reactant (Shown in Fig. 8b), it is evident that no CO<sub>2</sub> was present. This not only excludes TPA decomposition at the investigated temperature, but also strengthens the above-mentioned sublimation of TPA into the gas phase and out of the system. Figs. 2–5 also support this claim, since the CB loss of TPA is higher at experiments, where MeOH was removed during the reaction.

Similarly, as Yang and coworkers (Yang et al., 2022), we tested our solutions with NMR, to confirm selectivity and purity of the produced TPA. We observed peaks at 13.5 ppm (carboxyl proton) and 8.4 ppm (aromatic protons), along with a DMSO peak at 3 ppm (NMR spectra are in supplementary part of this paper). To mitigate water interference, we added a small amount of water to the TPA standard, causing the 13.5 ppm peak to vanish and a broad 5–6 ppm peak to emerge. MMT standard NMR mirrored TPA, with an additional 4.2 ppm peak, possibly from

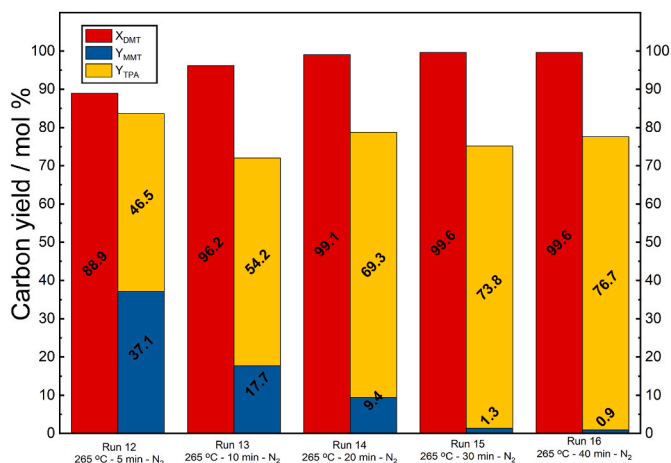


Fig. 5. Conversion of DMT and yields of MMT and TPA for experimental runs at 265 °C, with continuous removal of MeOH from the gas phase of the reactor.

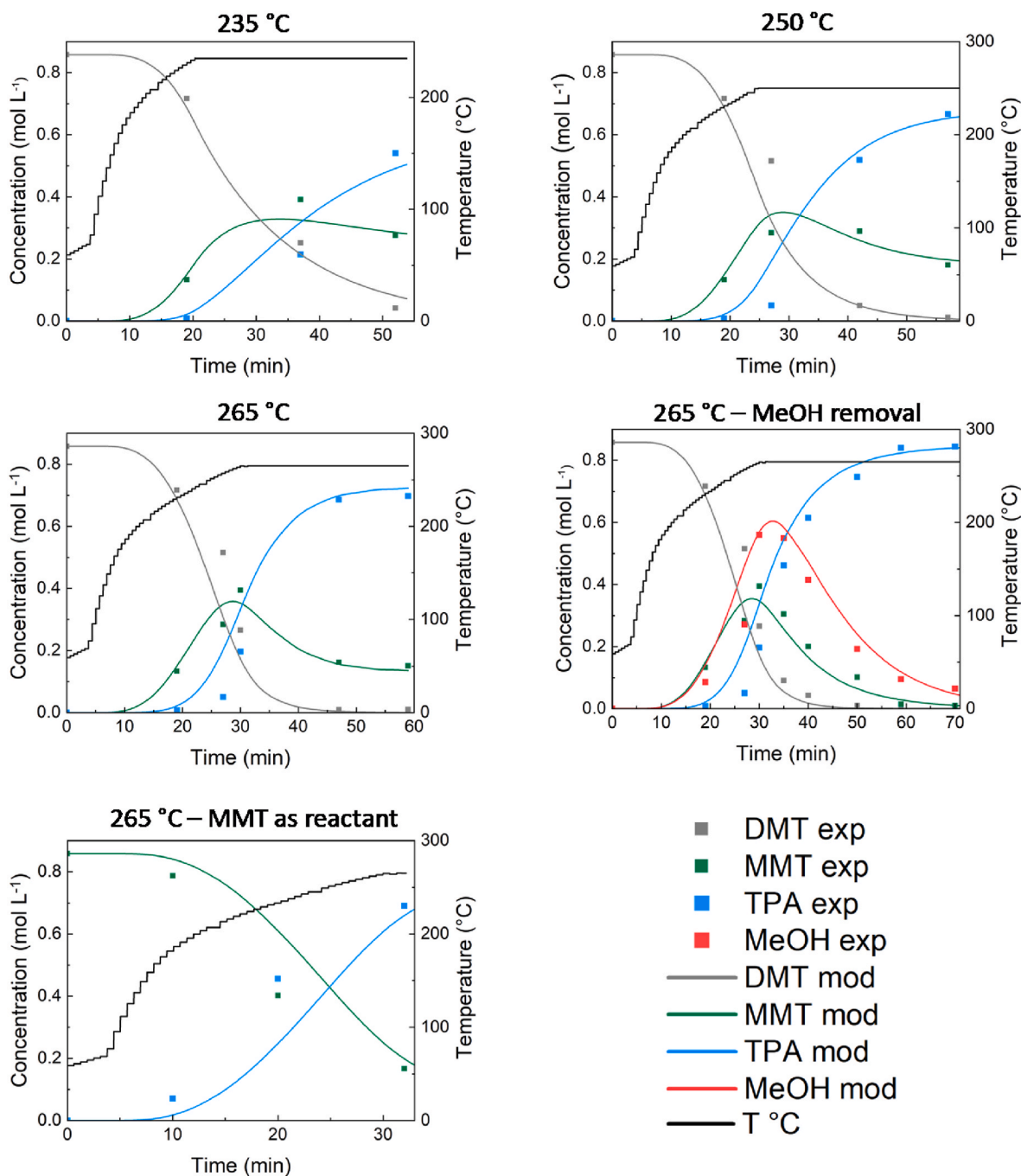


Fig. 6. Results of kinetic evaluation analysis of experimental data. Volume of liquid phase was 60 mL and 10 g of DMT or 9.3 g when MMT was used as reactant.

MMT or DMT methyl group hydrogen.

Experimental sample NMR spectra confirmed aromatic ring presence (8.4 ppm) and absence of the 13.5 ppm peak due to water. Notably, MeOH removal lowered MMT concentration, evident in a lower height of the 4.2 ppm peak. DMT samples displayed a 3.8 ppm peak, likely from an impurity in the stock material.

Interestingly, Colnik and coworkers (Čolnik et al., 2021; Liu et al., 2012) discovered decarboxylation reaction of TPA to benzoic acid, when they performed hydrolysis of PET. In their kinetic analysis, the degradation constant for TPA was determined to be  $0.00030 \pm 0.00036 \text{ min}^{-1}$  at 300 °C. Compared to our  $k_{26}$ , the degradation reaction is a 500-fold slower reaction. In addition to that, the predicted concentration profile of benzoic acid shows higher degradation, than experimentally determined values. To draw a conclusion, increasing the

temperature promotes the degradation of TPA, but the temperatures in our experiments did not exceed 265 °C, so the degradation to benzoic acid could not be determined.

As for the kinetic evaluation, the literature for this reaction is sparse. Sim et al. (Sim and Han, 2006) performed DMT hydrolysis using zinc acetate in a temperature range of 200–230 °C. After 8 h of reaction time, a TPA yield of 80% was obtained. When they calculated  $E_a$  for each reaction step,  $E_{a1}$  was surprisingly  $93 \text{ kJ mol}^{-1}$  and  $E_{a2}$  was  $63 \text{ kJ mol}^{-1}$ . Perhaps temperature has a greater effect on the hydrolysis of DMT and MMT than the addition of Zn acetate as a homogeneous catalyst. Another interesting study was carried out by Guo et al. (2022) using a HZSM-5 catalyst modified with Nb. Again, a lower temperature range (160–230 °C) and a reaction time of 2 h resulted in over 90 % conversion of DMT and a slightly lower TPA yield.

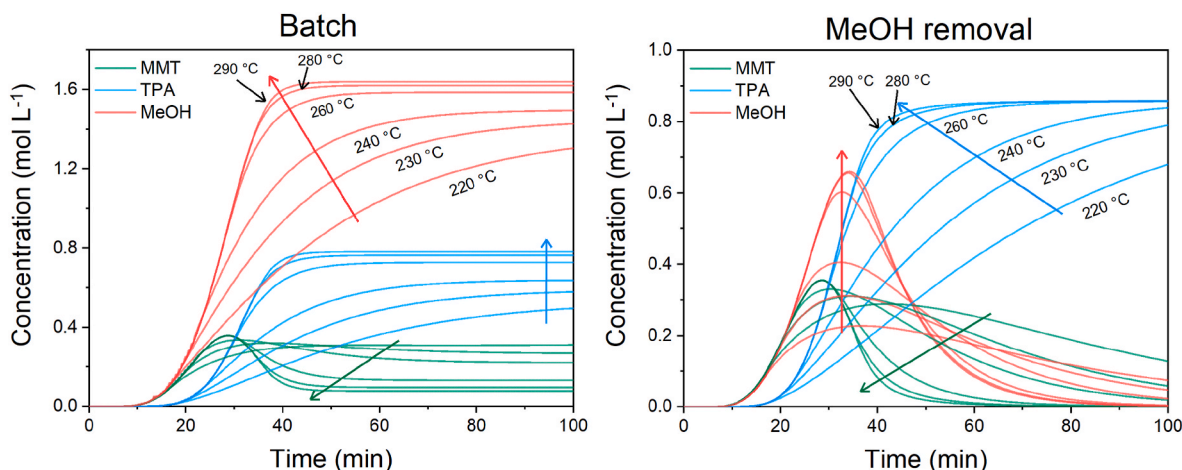


Fig. 7. Predicted concentration profiles for MMT, TPA and MeOH at various temperatures. Batch experiments without MeOH removal (left), and experiments with MeOH removal (right). The colored arrows show the change of each compound's concentration at different reaction temperatures.

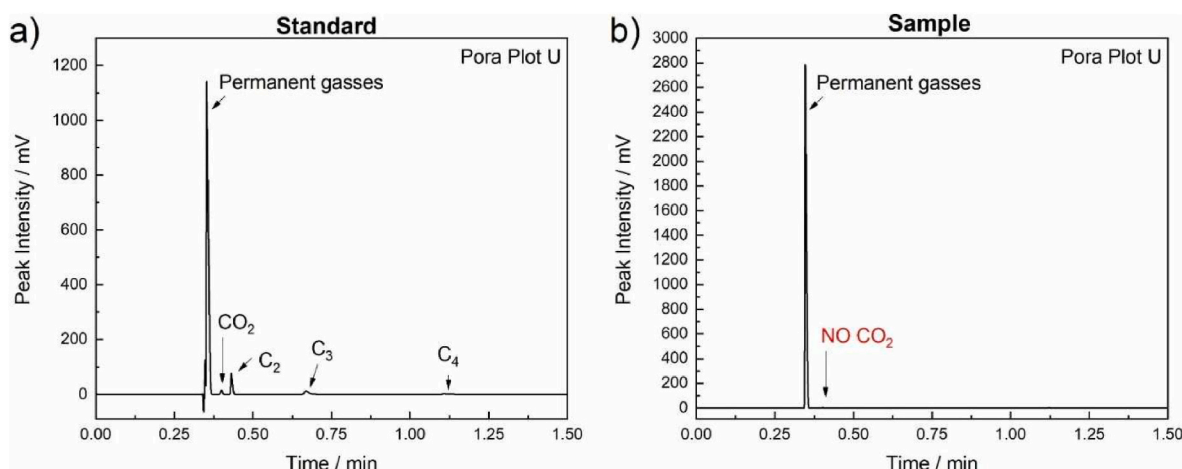


Fig. 8.  $\mu$ GC analysis of gas phase products after the reaction at 265 °C with TPA as reactant. Fig. 8a shows a chromatogram of a standard mixture containing CO<sub>2</sub> and various C<sub>2</sub>-C<sub>4</sub> gaseous products, while Fig. 8b shows chromatogram of a gas phase sample obtained after the TPA reaction.

Furthermore, we computed the comprehensive yield, spanning from PET methanolysis to DMT and subsequent DMT hydrolysis to TPA, leveraging conversions and yields sourced from Pudack and coworkers (Pudack et al., 2020). For an initial 1000 kg of PET material, the methanolysis process, boasting a 90 % DMT yield, generates 900 kg of DMT. However, achieving bottle-grade purity for TPA necessitates further purification before hydrolysis. This purification step, through re-crystallization, operates at a 95 % DMT yield, resulting in 855 kg of DMT from the initial 1000 kg of PET.

Upon removal of impurities, our analysis revealed a 91 % TPA yield when methanol (MeOH) is extracted from the solution, compared to a 75 % TPA yield when MeOH is retained (considering that yields, shown in Fig. 5, are lower due to inseparable TPA sublimation when MeOH is removed from the reaction mixture). Consequently, the overall yield from PET to TPA when MeOH is extracted stands at 78 %, contrasting with 64 % when MeOH is retained. Calculated per 1000 kg of initial PET material, the removal of MeOH yields an additional 140 kg of TPA. This is also presented in Table 3.

Considering the lower operating temperature at industrial scale, this would mean lower heating costs, while the costs for the catalytic material separation units and the separation itself need to be lower to compete with the uncatalyzed-high temperature process.

Table 3

Simulated mass balance for alcoholysis, DMT downstream processing and subsequent hydrolysis with and without MeOH removal.

PET start mass	1000 kg
PET alcoholysis conversion	90%
DMT mass after alcoholysis	900 kg
DMT stream cleaning from 97 to 99 % purity yield	95%
DMT mass after cleaning	855 kg
TPA yield hydrolysis with MeOH removal	91%
Produced mass of TPA	784 kg
Overall process yield	78%
TPA yield hydrolysis without MeOH removal	75%
Produced mass of TPA	644 kg
Overall process yield	64%
TPA mass difference between the two processes (with and without MeOH removal)	140 kg

## 5. Conclusion

In summary, the present study involved a successful experimental and kinetic modelling campaign to investigate hydrolysis reactions under vigorous reaction conditions. The results provided a crucial

insight: the hydrolysis of DMT to TPA is enhanced when MeOH is removed from the reaction mixture. When MeOH is removed from the reaction mixture, the selectivity of TPA is 25 % higher compared to the experiment, where MeOH is retained inside the reactor. When MeOH is removed from the reaction mixture, the concentration of MMT is insignificantly small compared to batch experiment without MeOH removal. In addition, our results showed that the TPA yield is lower at longer reaction times when MeOH is removed, possibly due to the sublimation of TPA.

Although batch reactive distillation proved to be beneficial for selectivity of TPA in our study, there are some crucial limitations. Intensive heating is required to reach the working temperature of 265 °C. This suggests a higher energy consumption, compared to a continuous production mode. The kinetic results from this study are beneficial to design a continuous process with steam stripping of MeOH from the reaction mixture, thereby improving the yield and final purity of produced TPA. Future work should include engineering of the separation unit, to improve water and MeOH separation and to prevent TPA sublimation. Furthermore, different reactor dimensions, purging gas inlet, the shape of impeller should be tested. Another important modification of the system would also be the continuous addition of DMT-water suspension and removal of produced TPA from the reaction mixture.

This study is the first to use experimentally derived values to construct a numerical kinetic model for DMT hydrolysis under catalyst-free conditions. The implications of our results are particularly important also in the context of the circular economy, as they demonstrate the feasibility of the final step of PET depolymerization - the production of high-purity monomer TPA - and the simultaneous generation of a valuable by-product, MeOH, which can be effectively isolated and recovered in a single step.

#### CRedit authorship contribution statement

**Žan Lavrič:** Writing – review & editing, Writing – original draft, Methodology, Investigation, Conceptualization. **Aleksa Kojčinović:** Writing – original draft, Methodology, Investigation, Conceptualization. **Irina Yarulina:** Writing – review & editing, Conceptualization. **Manfred Stepanski:** Writing – review & editing, Conceptualization. **Blaž Likozar:** Writing – review & editing, Supervision, Funding acquisition. **Miha Grilc:** Writing – review & editing, Supervision, Formal analysis, Conceptualization.

#### Declaration of competing interest

The authors declare that they have no known competing financial interests or personal relationships that could have appeared to influence the work reported in this paper.

#### Data availability

The data that has been used is confidential.

#### Acknowledgement

Ž.L., A.K., B.L. and M.G. sincerely acknowledge Sulzer Chemtech Ltd. for generous financial support and invaluable assistance with the conceptualization and proofreading of this work. Authors also acknowledge funding by Slovenian Research and Innovation Agency for research programs P2-0152 and I0-0003, as well as projects N2-0242 and J1-3020.

#### Appendix A. Supplementary data

Supplementary data to this article can be found online at <https://doi.org/10.1016/j.jclepro.2024.143867>.

#### References

- Aashish Mehra, 2023. Recycled PET market worth \$15.0 billion by 2028 - exclusive report by MarketsandMarkets™ [WWW Document]. <https://www.prnewswire.com/news-releases/recycled-pet-market-worth-15-0-billion-by-2028-exclusive-report-by-marketsandmarkets-301850464.html>, 8.8.24.
- Baliga, S., Wong, W.T., 1989. Depolymerization of poly(ethylene terephthalate) recycled from post-consumer soft-drink bottles. *J. Polym. Sci. Polym. Chem.* 27, 2071–2082. <https://doi.org/10.1002/pola.1989.080270625>.
- Benyathiar, P., Kumar, P., Carpenter, G., Brace, J., Mishra, D.K., 2022. Polyethylene terephthalate (PET) bottle-to-bottle recycling for the beverage industry: a review. *Polymers* 14, 2366. <https://doi.org/10.3390/polym14122366>.
- Chen, J.Y., Ou, C.F., Hu, Y.C., Lin, C.C., 1991. Depolymerization of poly(ethylene terephthalate) resin under pressure. *J. Appl. Polym. Sci.* 42, 1501–1507. <https://doi.org/10.1002/app.1991.070420603>.
- Čolnik, M., Pečar, D., Knez, Z., Goršek, A., Škerget, M., 2021. Kinetics study of hydrothermal degradation of PET waste into useful products. *Processes* 10, 24. <https://doi.org/10.3390/pr10010024>.
- Dimethyl Terephthalate (DMT), 2024. Polyethylene terephthalate (PET): navigating market changes & Innovations [WWW Document]. <https://mcgroup.co.uk/news/20240606/dimethyl-terephthalate-dmt-polyethylene-terephthalate-pet-navigating-market-changes-innovations.html>, 8.8.24.
- Elmas Kimyonok, A.B., Ulutürk, M., 2016. Determination of the thermal decomposition products of terephthalic acid by using curie-point pyrolyzer. *J. Energetic Mater.* 34, 113–122. <https://doi.org/10.1080/07370652.2015.1005773>.
- Genta, M., Iwaya, T., Sasaki, M., Goto, M., Hirose, T., 2005. Depolymerization mechanism of poly(ethylene terephthalate) in supercritical methanol. *Ind. Eng. Chem. Res.* 44, 3894–3900. <https://doi.org/10.1021/ie0488187>.
- Global recycled PET market - 2024-2031 [WWW Document]. <https://www.giiresearch.com/report/dmin1474058-global-recycled-pet-market.html>, 8.8.24.
- Guo, B., Liu, J., Tang, S., Liu, Y., Tian, Y., Lv, J., 2022. Hydrolysis of dimethyl terephthalate to terephthalic acid on Nb-modified <sc>HZSM</sc>-5 zeolite catalysts. *J. Chem. Technol. Biotechnol.* 97, 1695–1704. <https://doi.org/10.1002/jctb.7035>.
- Kim, B.-K., Hwang, G.-C., Bae, S.-Y., Yi, S.-C., Kumazawa, H., 2001. Depolymerization of polyethyleneterephthalate in supercritical methanol. *J. Appl. Polym. Sci.* 81, 2102–2108. <https://doi.org/10.1002/app.1645>.
- Kurokawa, H., Ohshima, M., Sugiyama, K., Miura, H., 2003. Methanolysis of polyethylene terephthalate (PET) in the presence of aluminium tiisopropoxide catalyst to form dimethyl terephthalate and ethylene glycol. *Polym Degrad Stab* 79, 529–533. [https://doi.org/10.1016/S0141-3910\(02\)00370-1](https://doi.org/10.1016/S0141-3910(02)00370-1).
- Liu, Y., Wang, M., Pan, Z., 2012. Catalytic depolymerization of polyethylene terephthalate in hot compressed water. *J. Supercrit. Fluids* 62, 226–231. <https://doi.org/10.1016/j.supflu.2011.11.001>.
- López-Fonseca, R., Duque-Ingunza, I., de Rivas, B., Arnaiz, S., Gutiérrez-Ortiz, J.I., 2010. Chemical recycling of post-consumer PET wastes by glycolysis in the presence of metal salts. *Polym Degrad Stab* 95, 1022–1028. <https://doi.org/10.1016/j.polymdegradstab.2010.03.007>.
- Neale, C.W., Hilyard, N.C., Barber, P., 1983. Observations on the economics of recycling industrial scrap plastic in new products. *Conserv. Recycl.* 6, 91–105. [https://doi.org/10.1016/0361-3658\(83\)90034-6](https://doi.org/10.1016/0361-3658(83)90034-6).
- Pudack, C., Stepanski, M., Fässler, P., 2020. PET recycling – contributions of crystallization to sustainability. *Chem. Ing. Tech.* 92, 452–458. <https://doi.org/10.1002/cite.201900085>.
- Sim, M., Han, M., 2006. Hydrolysis of dimethyl terephthalate for the production of terephthalic acid. *J. Chem. Eng. Jpn.* 39, 327–333. <https://doi.org/10.1252/jcej.39.327>.
- Sinha, V., Patel, M.R., Patel, J.V., 2010. Pet waste management by chemical recycling: a review. *J. Polym. Environ.* 18, 8–25. <https://doi.org/10.1007/s10924-008-0106-7>.
- Takebayashi, Y., Sue, K., Yoda, S., Hakuta, Y., Furuya, T., 2012. Solubility of terephthalic acid in subcritical water. *J. Chem. Eng. Data* 57, 1810–1816. <https://doi.org/10.1021/je300263z>.
- Yang, W., Wang, J., Jiao, L., Song, Y., Li, C., Hu, C., 2022. Easily recoverable and reusable p -toluenesulfonic acid for faster hydrolysis of waste polyethylene terephthalate. *Green Chem.* 24, 1362–1372. <https://doi.org/10.1039/D1GC04567A>.
- Zhang, H., Xia, Q., Yang, Y., Zhang, F.-B., Zhang, G.-L., 2013. Solubility of dimethyl terephthalate and monomethyl terephthalate in the methanol aqueous solution and its application to recycle monomethyl terephthalate from crude dimethyl terephthalate. *Ind. Eng. Chem. Res.* 52, 5230–5234. <https://doi.org/10.1021/ie400421e>.
- Zhu, M., Li, S., Li, Z., Lu, X., Zhang, S., 2012a. Investigation of solid catalysts for glycolysis of polyethylene terephthalate. *Chem. Eng. J.* 185–186, 168–177. <https://doi.org/10.1016/j.cej.2012.01.068>.
- Zhu, M., Li, Z., Wang, Q., Zhou, X., Lu, X., 2012b. Characterization of solid acid catalysts and their reactivity in the glycolysis of poly(ethylene terephthalate). *Ind. Eng. Chem. Res.* 51, 11659–11666. <https://doi.org/10.1021/ie300493w>.